Delayed-Decision-Feedback Equalization for Multiuser Systems

Ramon Schlagenhaufer*, Brent R. Petersen**, Abu B. Sesay*

* TR*Labs* / University of Calgary
280 Discovery Place One
3553 - 31 Str. N.W., Calgary, Alberta
CANADA T2L 2K7
e-mail: {schlagen,sesay}@cal.trlabs.ca

** Dept. of Electrical and Computer Engineering
University of New Brunswick
P.O. Box 4400 / Fredericton, New Brunswick
CANADA E3B 5A3
e-mail: b.petersen@ieee.org

Abstract— **The topic of this paper is delayed-decision-feedback equalization for wireless multiuser systems consisting of an arbitrary number of portables (users) and one central base station. The multiple users are supported by means of spread spectrum multiple access (SSMA) or CDMA. We consider joint or multiuser detection of all signals. In addition to bandwidth diversity, the system may employ antenna diversity at the receiver. The focus is on the reverse link. The radio channels are considered to be frequency selective. A flexible detection order of the multiple received signals is achieved by placing delay elements after the forward filters of the decision-feedback equalizer (DFE). This delays the signals of some users longer than those of others and results in different performance improvements for different users. The special cases of parallel and successive DFE result from no delays and infinite delays, respectively. These structures are analyzed and compared to the linear MMSE equalizer/combiner.**

Keywords— **Multiuser detection, decision feedback equalizers, interference suppression, diversity combining, wireless communication channel.**

I. INTRODUCTION

MANY wireless multiuser systems consist of several individual, spatially separated portables which communicate simultaneously with one base station. The realization of the reverse link, i.e. the transmission from the individual users to the base, is particularly difficult in systems based on spread spectrum multiple access (SSMA) or CDMA. Since the signal of different users may arrive in practice asynchronously, i.e. with different time delays, orthogonality of the received signals can not be guaranteed. This may cause severe interference at the base station which has to be mitigated with an appropriate receiver.

The strong increase in broadband applications necessitates high data rate systems. High symbol rates lead to frequency selective radio channels. Such an environment is extremely challenging because future, present and past symbols from all active portables distort a specific symbol of the user of interest. Additionally, these systems suffer from intersymbol interference (ISI), which also has to be mitigated.

The simplest SSMA receiver is a matched filter or rake receiver that is matched to the signal waveform of the desired signal. However, this detector does not take advantage of the underlying cyclostationarity of the interference caused by other signals and performs not very well in many situations. Moreover, the matched filter receiver is not near-far resistant and high-power interferers may cause a large error rate while detecting the signals of weaker users. On the other hand, the optimum detector [1] has been shown to be near-far resistant [2]. However, its complexity increases exponentially by the product of channel memory and the number of users. This prevents in many practical situations the use of the optimum detector, especially when there are many users in the system and/or the communications channel is highly frequency selective. Therefore, a lot of research has been conducted on suboptimal albeit near-far resistant multiuser receivers with a significantly better performance than the matched filter detector. The most promising receivers can be divided into equalizers and interference cancellers. The equalizer class comprises linear structures such as the decorrelating (zero-forcing) detector [3] and the MMSE equalizer/combiner [4], [5], [6] as well as

nonlinear decision-feedback detectors [7], [6], [8], [9], [10]. Interference cancellers (IC) are usually divided into parallel (PIC) [11] and successive (SIC) [12], [13] structures.

This paper concentrates on the class of multiuser decision-feedback equalizers (DFE) which use the symbols of all detected signals in the feedback process [6], [9]. Comparing these detectors to interference cancellers, the current DFE structures can be described as parallel detectors. Both types of receivers make the decisions on multiple data sequences predominantly in parallel[1], i.e. symbols sent at the same time are detected at approximately the same time. Consequently, the received signals are not delayed with respect to each other in the detector. As a result, the received sequences of all users benefit on average almost equally from the decision-feedback and interference reduction procedures. Research results in multistage interference cancellation and recent work on multiuser DFE receivers [10] show that this method is particularly effective in situations when the received powers of all users differ only slightly (which may be achieved with effective power control techniques). In practice, however, the power of the received signals turns out to vary considerably unless power control techniques are applied. As a result, weak signals tend to be detected with a considerably poorer error performance than stronger signals. It is thus the weak signals that limit the overall system performance. One possible strategy would be to concentrate in the signal enhancement through decision-feedback as much as possible on the weak users while sacrificing a possible improvement of the stronger signals. This leads to the successive DFE receivers which detect the signals according to their received power. All symbols of the strongest signal are detected first. These decisions are then used in the feedback filter to improve the performance of the second strongest signal, and so on. Finally, for the detection of the weakest user's symbols, the transmitted data of all other users is known. This knowledge enables the best possible performance enhancement of the weakest signal.

A successive multiuser DFE for frequency selective

environments has been introduced only recently [10]. In fact, the described multivariate noise-predictive delayed-decision-feedback equalizer (MNP-DDFE) allows a much more flexible detection order than only parallel or successive. The behavior of the MNP-DDFE depends on the choice of delay elements which delay the pre-equalized signals of the different users. The MNP-DDFE reduces for the special case of no delays between different signals to the conventional parallel DFE structures. Introducing very long delays between the received signals of two consecutive users results in a successive DFE. In general, other choices for the delay parameters realize detectors that may be described as compromise between purely parallel and successive.

The general idea of delayed-decision-feedback equalization is the topic of this paper. We start out in Section II with the definition of the system model. This model is very general. It allows an arbitrary number of N users to access the system. The use of diversity techniques such as bandwidth diversity and antenna diversity at the receiver is optional. Theoretical and numerical results [14], [15], [16], [17] suggest that the number of system users be smaller than the product of processing gain and number of receive antennas in order to achieve acceptable performance. The description of the equalizer is kept general. It comprises the classes of linear and decision-feedback equalizers. The general equalizer structure is discussed and the linear MMSE equalizer/combiner (E/C) is derived. It is shown that the MMSE E/C may be realized by a noise-whitening, a matched filter and a symbol rate equalizer part. An equivalent discrete-time model of the complete system is derived and expressed in compact matrix notation. Section III discusses multiuser decision-feedback equalizers. The DFE receivers are symbol-by-symbol detectors. In multiuser systems, the order in which the decisions are made becomes an important issue. The concept of the *decision path* is introduced. Different implementations of the delayed DFE detector are described. The noise-predictive version is analyzed in more detail. We concentrate then on the analysis of the successive DFE structure. It is shown that the feedforward filter is identical to the linear MMSE E/C and that there are no matrix inversions required in the calculation of the feedback filter. This suggests that the parameters of the successive DFE may be computed very efficiently when compared to the general DFE receiver with arbitrary delays. Finally, numerical results comparing the linear MMSE E/C, successive and parallel delayed DFE detectors are shown in Section IV.

---

[1]So far, research work has mostly been done for systems in which the cochannel interference (CCI) comes only from symbols sent at the same time. For example, the multiuser DFE structure used by Duel-Hallen [8] does not delay the individual signals and processes the users according to their received signal power. Thus, this structure is certainly a successive receiver. Note, however, that we consider a system with a strongly frequency selective channel in which the cochannel interference (CCI) stems in general from past, present and future symbols. In such an environment, processing over the user order only does not result in a successive receiver since the CCI from future symbols of the stronger users can not be estimated.

Fig. 1. Block diagram of the multiuser system.

II. SYSTEM MODEL

Consider the reverse link of a wireless multiuser system with N portables and one central base station. The portables are equipped with one antenna each, and the base station receives the signals at A different antennas. Figure 1 shows the block diagram of the multiuser system.

The complex baseband notation is used to describe the system. All signals and impulse responses are in general complex functions. The N users transmit the data sequences a_i $(i = 1, \ldots, N)$. Each data sequence consists of symbols drawn from a finite alphabet of complex numbers $(a_i[n] \in \mathcal{A})$. After K times upsampling, the individual sequences are filtered by discrete-time filters q_i. Their outputs are fed into linear impulse generators which modulate the discrete-time sequences with the waveform $p_C(t)$ to produce the transmit signals. Let the clock rate of the impulse generators be $1/T_s$. The symbol period is then given by $T = KT_s$.

The signal of user i travels through the radio channel with impulse response $h_{Cil}(t)$ and is received at antenna l of the base station. Mutually independent, complex AWGN signals ν_{CGl} $(l = 1, \ldots, A)$ with two-sided power spectral density N_0 are added at each of the A base station antennas. The received signals are lowpass filtered ($b_C(t)$), sampled at a rate $1/T_s$ and fed into an equalizer with A inputs and N outputs. The final output signals $\hat{a}_k$ $(k = 1, \ldots, N)$ are quantized estimates of the input sequences a_i. Both the input and output signals belong to the same finite alphabet $(\hat{a}_k[n] \in \mathcal{A})$.

Consider the *net channel* between user i and the l-th receive antenna which is given by the convolution of $p_C(t)$, $h_{Cil}(t)$ and $b_C(t)$:

$$\psi_{Cil}(t) = \iint_{-\infty}^{\infty} p_C(u) h_{Cil}(v - u) b_C(t - v) \, du \, dv. \tag{1}$$

After sampling, the noise signal components are colored because of the influence of the receive filters b_C:

$$\nu_l[n] = \int_{-\infty}^{\infty} b_C(\tau) \nu_{CGl}(nT_s - \tau) \, d\tau. \tag{2}$$

The continuous-time net channel is embedded into the overall discrete-time system. It can be described by equivalent discrete-time impulse responses $\psi_{il}[n] = \psi_{Cil}(nT_s)$. Let us define the *combined channel*

$$x_{il}[n] = \sum_{v=-\infty}^{\infty} q_i[v] \psi_{il}[n - v]. \tag{3}$$

The analysis is done using the D-transform which is defined by $\boldsymbol{u}(D) = \sum_{n=-\infty}^{\infty} \boldsymbol{u}[n] D^n$, where $\boldsymbol{u}$ may be an arbitrary dimensional row vector $\boldsymbol{u} = [u_1, u_2, \ldots]$. Let us define the truncated sequence

$$\boldsymbol{u}_M[n] = \begin{cases} \boldsymbol{u}[n] & \text{, for } |n| \leq M \\ 0 & \text{, for } |n| > M. \end{cases} \tag{4}$$

Let $\boldsymbol{v}$ be another row vector whose truncated sequence is defined according to Equation (4). The cross-power spectrum $\boldsymbol{S}_{uv}(D)$ of $\boldsymbol{u}[n]$ and $\boldsymbol{v}[n]$ is then equal to

$$E_M[\boldsymbol{u}^H(D^{-*}) \boldsymbol{v}(D)] \stackrel{\text{def}}{=} \lim_{M \to \infty} \frac{E[\boldsymbol{u}_M^H(D^{-*}) \boldsymbol{v}_M(D)]}{2M + 1} \tag{5}$$

where 'E' is the expectation operator, the superscripts 'H', '*', '−1' denote the conjugate transpose, complex conjugate and inverse, respectively. The superscript '−*' shall be interpreted in the sense $D^{-*} = (D^{-1})^*$.

According to Figure 1 the input signals y_l $(l = 1, \ldots, A)$ to the $A \times N$ equalizer can be written as

$$s_i(D) = a_i(D^K) \tag{6}$$

$$y_l(D) = \sum_{i=1}^{N} s_i(D) x_{il}(D) + \nu_l(D). \tag{7}$$

Let us express the signals in vector form and introduce the channel matrix $\boldsymbol{X}$:

$$\boldsymbol{a}(D) = [a_1(D), a_2(D), \ldots, a_N(D)] \tag{8}$$

$$\hat{\boldsymbol{a}}(D) = [\hat{a}_1(D), \hat{a}_2(D), \ldots, \hat{a}_N(D)] \tag{9}$$

$$\boldsymbol{y}(D) = [y_1(D), y_2(D), \ldots, y_A(D)] \tag{10}$$

$$\boldsymbol{\nu}(D) = [\nu_1(D), \nu_2(D), \ldots, \nu_A(D)] \tag{11}$$

$$\boldsymbol{X}(D) = \begin{bmatrix} x_{11}(D) & \ldots & x_{1A}(D) \\ \vdots & \ddots & \vdots \\ x_{N1}(D) & \ldots & x_{NA}(D) \end{bmatrix}. \tag{12}$$

(a) General equalizer structure

(b) Equivalent linear equalizer model
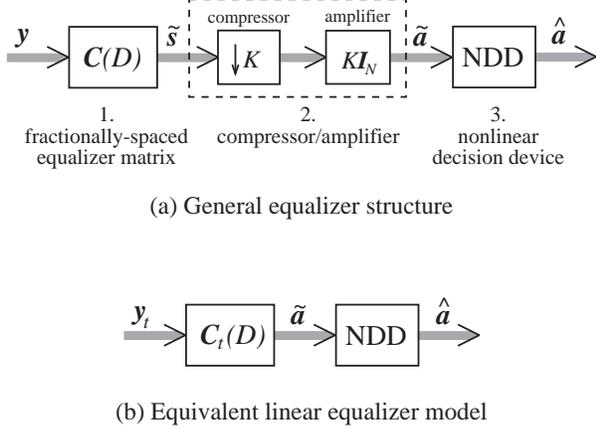
Fig. 2. General equalizer structure and equivalent model.

A. General Equalizer Structure

The general structure of the $A \times N$ equalizer is detailed in Figure 2(a). It consists of a linear fractionally-spaced forward filter matrix $\boldsymbol{C}$ with A inputs and N output signals $\tilde{s}_k$ ($k = 1, \ldots, N$). The sequences $\tilde{s}_k$ are downsampled K times by compressors and amplified with gain K. $\boldsymbol{I}_N$ denotes the $N \times N$ identity matrix. The amplifier output $\tilde{a}_k$ constitutes a preliminary linear estimate of user k's input signal a_k. The samples $\tilde{a}_k[n]$ are continuous-valued complex numbers. In the last step, a non-linear decision device (NDD) is used to produce the quantized estimates $\hat{a}_k$.

Again, the scalar sequences are combined into vector and matrix form:

$$\tilde{\boldsymbol{s}}(D) = [\tilde{s}_1(D), \tilde{s}_2(D), \ldots, \tilde{s}_N(D)] \qquad (13)$$

$$\tilde{\boldsymbol{a}}(D) = [\tilde{a}_1(D), \tilde{a}_2(D), \ldots, \tilde{a}_N(D)] \qquad (14)$$

$$\boldsymbol{C}(D) = \begin{bmatrix} c_{11}(D) & \ldots & c_{1N}(D) \\ \vdots & \ddots & \vdots \\ c_{A1}(D) & \ldots & c_{AN}(D) \end{bmatrix} \qquad (15)$$

where $c_{lk}(D)$ is the transfer function from input l to output k of $\boldsymbol{C}$. The transfer function and corresponding impulse response $c_{lk}[n]$ are connected through the D-transform. It can easily be verified that the output signals of the forward filter $\boldsymbol{C}$ and the amplifier are given by

$$\tilde{s}_k(D) = \sum_{l=1}^{A} y_l(D) c_{lk}(D) \qquad (16)$$

$$\tilde{a}_k(D) = \sum_{m=0}^{K-1} \tilde{s}_k(D^{\frac{1}{K}} w_K^m) \qquad (17)$$

where $w_K = e^{-j2\pi/K}$.

In order to derive an equivalent model of the equalizer structure in Figure 2(a), the extended signal vectors and channel matrix are defined as

$$\boldsymbol{y}_t(D) = [\boldsymbol{y}(\gamma_0), \boldsymbol{y}(\gamma_1), \ldots, \boldsymbol{y}(\gamma_{K-1})] \qquad (18)$$

$$\boldsymbol{\nu}_t(D) = [\boldsymbol{\nu}(\gamma_0), \boldsymbol{\nu}(\gamma_1), \ldots, \boldsymbol{\nu}(\gamma_{K-1})] \qquad (19)$$

$$\boldsymbol{X}_t(D) = [\boldsymbol{X}(\gamma_0), \boldsymbol{X}(\gamma_1), \ldots, \boldsymbol{X}(\gamma_{K-1})] \qquad (20)$$

$$\boldsymbol{C}_t(D) = [\boldsymbol{C}^H(\gamma_0), \boldsymbol{C}^H(\gamma_1), \ldots, \boldsymbol{C}^H(\gamma_{K-1})]^H \qquad (21)$$

where $\gamma_m = D^{\frac{1}{K}} w_K^m$. Using these definitions together with Equations (6), (7), (16) and (17), the extended equalizer input signal $\boldsymbol{y}_t$ and the linear estimate $\tilde{\boldsymbol{a}}$ can be expressed as

$$\boldsymbol{y}_t(D) = \boldsymbol{a}(D) \boldsymbol{X}_t(D) + \boldsymbol{\nu}_t(D) \qquad (22)$$

$$\tilde{\boldsymbol{a}}(D) = \boldsymbol{y}_t(D) \boldsymbol{C}_t(D) \qquad (23)$$

where we used the fact that $w_K^{Km} = 1$ if m is an integer. The general equalizer structure in Figure 2(a) may therefore be described equivalently by the model shown in Figure 2(b). In the equivalent equalizer model, we replace the filter matrix $\boldsymbol{C}$, downsampler and amplifier by the extended forward filter matrix $\boldsymbol{C}_t$. Additionally, the input $\boldsymbol{y}$ is replaced by the extended signal $\boldsymbol{y}_t$.

Note that the vector signal $\boldsymbol{y}_t$ contains AK scalar signals that can be used to estimate the N system input signals contained in $\boldsymbol{a}$. Obviously, the input data can only be accurately estimated if there are at least as many equalizer input signals as system input signals. A necessary condition for the successful estimation is therefore that the number of system users (N) is smaller or equal to the product of processing gain (K) and number of receive antennas (A):

$$N \leq AK. \qquad (24)$$

B. Spectral Correlation of the Noise

For the results derived in the following section we need an expression for the matrix spectrum of the noise vector $\boldsymbol{\nu}_t(D)$. Let $\boldsymbol{S}_n$ be the spectrum of the additive Gaussian noise (AGN) signal $\boldsymbol{\nu}$: $\boldsymbol{S}_n(D) = E_M[\boldsymbol{\nu}^H(D^{-*}) \boldsymbol{\nu}(D)]$ where the operator 'E_M' is defined in Eqn. (5). The receive filters $b_C(t)$ introduce correlation between noise signal symbols at the input of the samplers. Let $B(f) = \int_{-\infty}^{\infty} b_C(t) e^{-j2\pi ft} \, dt$ denote the transfer function of the receive filters. Since the analog filters $b_C(t)$ are identical at each receiver input, it can be shown that the spectrum of the AGN signal is given by

$$\boldsymbol{S}_n(D) = \frac{N_0}{T_s} \left(\sum_{v=-\infty}^{\infty} |B(f - v/T_s)|^2 \right) \boldsymbol{I}_A \qquad (25)$$

with $D = e^{-j2\pi\check{f}}$ and $\check{f} = fT_s$. N_0 is the power spectral density of the AWGN signals ν_{CGl} and $\boldsymbol{I}_A$ is the $A \times A$ identity matrix. It was assumed in the derivation of Eqn. (25) that the noise signals at different receiver inputs are mutually independent and that the spectral components of the signals ν_{CGl} are uncorrelated if they are separated by at least $\Delta f = 1/T_s$.

Let us define the spectrum of the extended noise signal $\boldsymbol{\nu}_t$ as $\boldsymbol{S}_\nu(D) = E_M[\boldsymbol{\nu}_t^H(D^{-*})\boldsymbol{\nu}_t(D)]$. Using the result in (25) it can be shown that $\boldsymbol{S}_\nu(D)$ is given by

$$\boldsymbol{S}_\nu(D) = K\,\mathbf{Diag}\langle\boldsymbol{S}_n(D^{\frac{1}{K}}w_K^m)\rangle,\ m = 0,\dots,K{-}1 \tag{26}$$

where $\mathbf{Diag}\langle\boldsymbol{G}_i\rangle$ is a diagonal hypermatrix with diagonal elements $\boldsymbol{G}_i$ $(i = 1,2,\dots)$, which may be matrices of arbitrary size. Since $\boldsymbol{S}_n(D)$ is a $A \times A$ diagonal matrix with nonnegative elements, (25), $\boldsymbol{S}_\nu(D)$ is a $AK \times AK$ diagonal matrix with nonnegative elements. It is reasonable to assume that all diagonal elements are nonzero. In this case, $\boldsymbol{S}_\nu(D)$ is positive definite.

C. Linear MMSE Equalizer/Combiner

For a linear receiver the nonlinear decision device (NDD) is identical to N single-input single-output quantizers. Each of them is connected to one of the outputs of the linear forward filter matrix.

According to Equation (23) the linear MMSE estimate $\tilde{\boldsymbol{a}}(D)$ can immediately be determined by multiplying the extended equalizer input signal $\boldsymbol{y}_t(D)$ with the extended forward filter matrix $\boldsymbol{C}_t(D)$ (Figure 3(a)). Alternatively, the optimum linear MMSE equalizer/combiner (E/C) can also be realized by decomposing $\boldsymbol{C}_t(D)$ into [17] [2]

$$\boldsymbol{C}_t(D) = \boldsymbol{S}_\nu^{-1}(D)\boldsymbol{X}_t^H(D^{-*})\boldsymbol{L}(D) \tag{27}$$

where $\boldsymbol{L}(D)$ is an $N \times N$ matrix depending on D. A block diagram of this structure is shown in Figure 3(b).

Let the input signal to the filter matrix $\boldsymbol{L}(D)$ be $\boldsymbol{u}(D) = \boldsymbol{y}_t(D)\boldsymbol{S}_\nu^{-1}(D)\boldsymbol{X}_t^H(D^{-*})$. Expanding this expression using Equations (18), (20) and (26), it can easily be shown that $\boldsymbol{u}(D)$ may be written as

$$\boldsymbol{u}(D) = \frac{1}{K}\sum_{m=0}^{K-1}\boldsymbol{y}(\gamma_m)\boldsymbol{S}_n^{-1}(\gamma_m)\boldsymbol{X}^H(\gamma_{m*}) \tag{28}$$

[2]The expressions for $\boldsymbol{C}_t$ in Reference [17] and Eqn. (27) differ by a factor K. This is the result of different expressions for $\tilde{\boldsymbol{a}}(D)$ in Ref. [17] and Eqn. (23), which differ also by a factor of K.
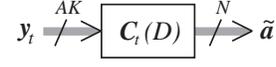
(a) Direct structure
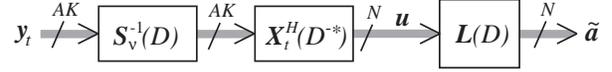
(b) Extended structure

Fig. 3. Structures for the optimum MMSE equalizer/combiner.
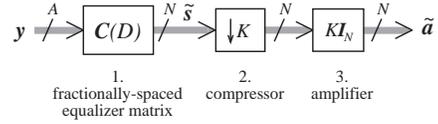
(a) General equalizer structure
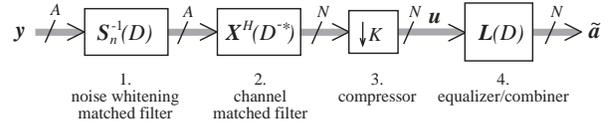
(b) Alternative structure

Fig. 4. Possible implementations of the optimum MMSE equalizer/combiner.

with $\gamma_m = D^{\frac{1}{K}}w_K^m$ and $\gamma_{m*} = (D^{-*})^{\frac{1}{K}}w_K^m$. This equation shows that the signal $\boldsymbol{u}$ may be generated by a system consisting of three elements. The first is a noise whitening matched filter matrix with transfer function $\boldsymbol{S}_n^{-1}(D)$, which is the inverse of the noise spectrum matrix (25). It is followed by the matched filter matrix $\boldsymbol{X}^H(D^{-*})$ which is matched to the combined discrete-time channels (3). The last element is a compressor that downsamples all signals by a factor K. The resulting signal $\boldsymbol{u}[n]$ is a symbol-spaced sequence. Finally, the filter matrix $\boldsymbol{L}(D)$ produces the linear estimate $\tilde{\boldsymbol{a}}$.

Figure 4 shows two possible implementations of the linear filter matrix $\boldsymbol{C}_t(D)$. The first solution (a) is identical to the general equalizer structure also shown in Figure 2(a). The second block diagram (b) shows the alternative structure derived above.

It can be shown, [17], [5], [6], that the filter matrix of the optimum MMSE E/C is given by

$$\boldsymbol{L}(D) = [\boldsymbol{S}_a(D)\boldsymbol{S}_x(D) + \boldsymbol{I}_N]^{-1}\boldsymbol{S}_a(D) \tag{29}$$

where $\boldsymbol{S}_a(D)$ is the spectrum of the input signal and

$\boldsymbol{S}_x(D)$ is the *effective channel*

$$\boldsymbol{S}_a(D) = E_M[\boldsymbol{a}^H(D^{-*})\boldsymbol{a}(D)] \qquad (30)$$

$$\boldsymbol{S}_x(D) = \boldsymbol{X}_t(D)\boldsymbol{S}_\nu^{-1}(D)\boldsymbol{X}_t^H(D^{-*}). \qquad (31)$$

An expression for the minimum mean-squared error (MMSE) of the linear MMSE E/C is given in the following. Let us assume that the input signals a_i of different users are mutually independent and that samples of the same sequence are uncorrelated with zero mean and variance $\mathcal{E}_a$:

$$E\left[a_i[n]a_k[m]\right] = \mathcal{E}_a\delta[i-k]\delta[n-m] \qquad (32)$$

where $\delta[k]$ is the Kronecker delta sequence. In this case, the spectrum of the input signal reduces to

$$\boldsymbol{S}_a(D) = \mathcal{E}_a\,\boldsymbol{I}_N. \qquad (33)$$

The *normalized* MMSE (NMMSE) of the k-th user is defined as

$$\sigma_{\mathrm{lin},k} = 1/\mathcal{E}_a\,E\left[|\tilde{a}_k[n] - a_k[n]|^2\right]. \qquad (34)$$

It can then be shown, [6], [17], [10], that the NMMSE for user k is given by

$$\sigma_{\mathrm{lin},k} = \frac{1}{\mathcal{E}_a}\int_0^1 L_{kk}(e^{-j2\pi\check{f}})\,d\check{f} \qquad (35)$$

where $L_{kk}(D)$ is the k-th diagonal element of the matrix $\boldsymbol{L}(D)$ from Eqn. (29).

D. Equivalent Discrete-Time Model

An equivalent discrete-time system model is obtained by combining the system block digram shown in Figure 1 and the optimum structure of the linear MMSE E/C in Figure 3(b). Figure 5(a) shows the extended structure of the discrete-time model. $\boldsymbol{W}(D)$ is a linear $N \times N$ matrix filter. It is chosen such that the mean-squared error (MSE) at the output is minimized. In general, $\boldsymbol{W}(D)$ depends on the structure of the nonlinear decision device (NDD). In case of the linear MMSE E/C, we have to choose $\boldsymbol{W}(D) = \boldsymbol{L}(D)$ in order to minimize the MSE.

The channel of the equivalent model is the effective channel $\boldsymbol{S}_x(D)$ which consists of the combined channel $\boldsymbol{X}(D)$, the whitening matched filter matrix $\boldsymbol{S}_\nu^{-1}(D)$ and the channel matched filter matrix $\boldsymbol{X}_t^H(D^{-*})$. It is easily verified that the effective channel is an N-input N-output symbol-spaced discrete-time system. The continuous-time noise signals ν_{CGl} added in front of the receive filters $b_C(t)$ are equivalently replaced by a symbol rate discrete-time noise vector $\boldsymbol{z}$ added after $\boldsymbol{S}_x$:

$$\boldsymbol{z}(D) = \boldsymbol{\nu}_t(D)\boldsymbol{S}_\nu^{-1}(D)\boldsymbol{X}_t^H(D^{-*}). \qquad (36)$$
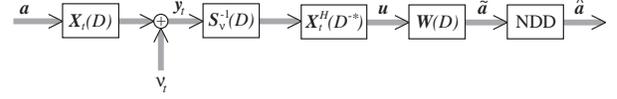
(a) Extended discrete-time model
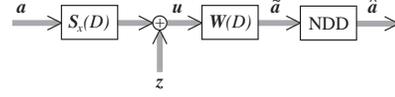
(b) Equivalent discrete-time model

Fig. 5. Discrete-time model of the system.

As easily verified, the spectrum of this noise signal is given by

$$\boldsymbol{S}_z(D) = E_M[\boldsymbol{z}^H(D^{-*})\boldsymbol{z}(D)] = \boldsymbol{S}_x(D). \qquad (37)$$

It is worth noting that the spectrum of the noise is identical to the transfer function of the effective channel. This is not an assumption but rather a result of described model.

Let us assume that the input sequences a_i and the continuous-time noise signals ν_{CGl} ($i = 1, \ldots, N;\ l = 1, \ldots, A$) are uncorrelated and that the noise signals have zero mean. The cross-spectrum of the input and discrete-time noise is then zero:

$$\boldsymbol{S}_{az}(D) = E_M[\boldsymbol{a}^H(D^{-*})\boldsymbol{z}(D)] = \boldsymbol{O}_N \qquad (38)$$

where $\boldsymbol{O}_v$ is the $v \times v$ zero matrix.

A simple but equivalent discrete-time model is shown in Figure 5(b). It consists only of an $N \times N$ channel matrix, additive discrete-time noise $\boldsymbol{z}$ and the receiver. The receiver itself can be divided into a linear $N \times N$ filter matrix $\boldsymbol{W}(D)$ and a nonlinear decision device.

III. DECISION-FEEDBACK EQUALIZERS

Decision-feedback equalizers (DFE) use already detected symbols in a feedback procedure in order to improve the quality of the signals at the input to the quantizers. Formally, the feedback loops can be included into the nonlinear decision device (NDD). Only previously detected symbols may be used in the feedback process because of causality constraints. Note that, in general, previously detected symbols are not necessarily identical to previously transmitted or received symbols. Therefore, the order in which the decisions are made may affect the performance of the DFE significantly.

A. Decision Path

Let us define the *decision path* as the order in which the final decisions on the symbols are made.

Consider at first the single user case. The input to the decision quantizer is the scalar signal $\bar{\alpha}[n]$. The natural way to perform the symbol-by-symbol decisions is in chronological order, i.e. quantizing at first the symbol $\bar{\alpha}[n]$, then $\bar{\alpha}[n + 1]$, after that $\bar{\alpha}[n + 2]$, and so on. The decision path goes in this case successively from $n = -\infty$ to $n = \infty$. In general, the decision path may be chosen arbitrarily. For example, we could, by modifying the equalizer structure appropriately, perform the decisions in the following order: $\bar{\alpha}[0], \bar{\alpha}[2], \bar{\alpha}[1], \bar{\alpha}[3], \dots$. However, the chronological decision path has been preferred in the literature. Let us describe the decision path with the *decision order function* $d[n]$. This function maps the symbol index n into an integer number. The value of d shall be interpreted as the decision index, i.e. the $d[n_0]$-th decision is made on the symbol $\bar{\alpha}[n_0]$. For the chronological decision order, d might be expressed as $d[n] = n$.

Consider now a multiuser system with N users. Let us express the signal to be quantized as two-dimensional scalar function $\bar{\alpha}[n, k]$, where n is the time index and k is the user number. The decision path can now be chosen arbitrarily in the $[n, k]$-plane. This is described with a two-dimensional decision order function $d[n, k]$.

As a special case, we might choose to perform the decisions at first with respect to the users and afterwards with respect to time. Figure 6 shows the decision path for a system with 4 users and sequences of length 4. The horizontal direction represents the time dimension and the different users are ordered vertically. Each circle represents a symbol at the input to the decider. The values of the decision order function d are printed inside the circles. The detection of the different sequences is performed almost in parallel. Therefore, this decision order is referred to as *parallel*.

When the whole sequences are detected subsequently, the decision order is called *successive*. In this case the decision path is chosen as shown in Figure 7. For infinite-length sequences, at first the symbols of sequence 1 are detected for all times $n \in (-\infty, \infty)$. After that all symbols of sequence 2 are detected, and so on, until all sequences are quantized. Note that for the decision of symbol $\bar{\alpha}[n_0, k_0]$ *all* symbols of the sequences k for $k < k_0$ are available and may be used in the feedback loop. Also available are all temporally preceding symbols of the same sequence, i.e. the symbols $\bar{\alpha}[n, k_0]$ for $n < n_0$.
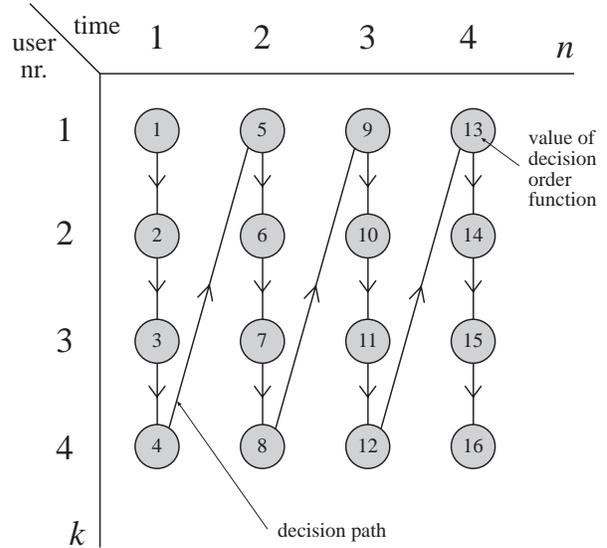
Fig. 6. Decision path for parallel decision order in a system with 4 users and 4 symbols per user.
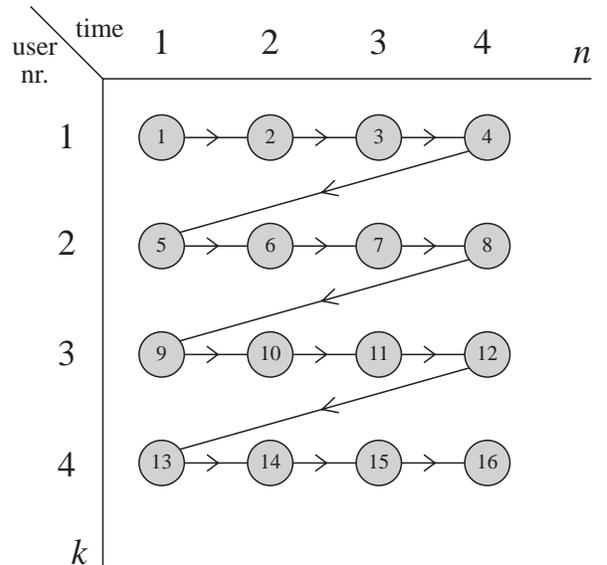
Fig. 7. Decision path for successive decision order in a system with 4 users and 4 symbols per user.

B. Delayed DFE Structures

The conventional DFE structures for multiuser systems are parallel detectors [18], [6], [9]. Their decision order is strictly defined and cannot be changed. A more flexible detection order can be achieved by including delay elements after the linear forward filter matrix [10]. It was shown that a change in the detection order strongly affected the results in certain situations. More specifically, it was shown that a more successive detection order performed significantly better than a parallel DFE if
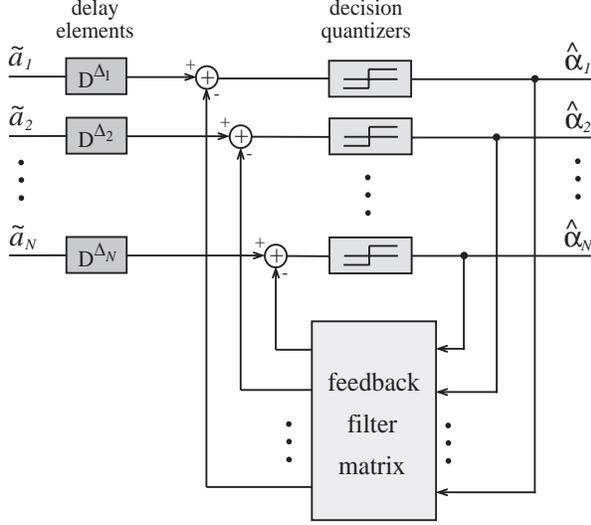
Fig. 8. Nonlinear decision device (NDD) of the M-DDFE.

Fig. 9. Nonlinear decision device (NDD) of the MNP-DDFE.
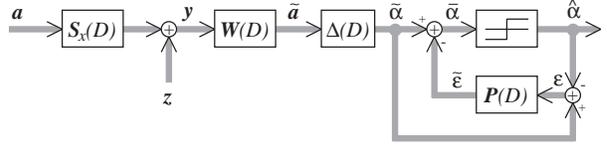
Fig. 10. Equivalent discrete-time system model of the MNP-DDFE.

the power of the received signals varied by up to 10 dB.

C. M-DDFE

The multivariate delayed-decision-feedback equalizer (M-DDFE) is an extension of the conventional multivariate DFE [6]. It is obtained by inserting one delay element at every output of the forward filter matrix $\boldsymbol{W}$. The structure of the nonlinear decision device (NDD) is shown in Figure 8. Each decision element D^{Δ_k} $(k = 1, 2, \ldots, N)$ delays the input sequence by Δ_k symbols, where Δ_k may be an arbitrary nonnegative integer number.

D. MNP-DDFE

We investigate in this section the multivariate noise-predictive delayed-decision-feedback equalizer (MNP-DDFE) [10]. This receiver, which is obtained by including delay elements at the input of the NDD, is an extension of the multivariate noise-predictive DFE [9]. Figure 9 shows the NDD structure of the MNP-DDFE. The delay elements are represented by blocks with transfer functions D^{Δ_k}, which delay the input signal by Δ_k symbols $(k = 1, 2, \ldots, N)$. Incorporating the NDD into the equivalent discrete-time model results in the overall system model (Figure 10). The delay elements are now described by the *delay matrix*

$$\boldsymbol{\Delta}(D) = \mathbf{Diag}\langle D^{\Delta_k}\rangle, \quad k = 1, 2, \ldots, N \quad (39)$$

where $\mathbf{Diag}\langle u_i\rangle$ is a diagonal matrix with diagonal elements u_i $(i = 1, 2, \ldots)$. The output of the delay matrix

$$\tilde{\boldsymbol{\alpha}} = \tilde{\boldsymbol{a}}(D)\boldsymbol{\Delta}(D) \quad (40)$$

is subtracted from the decisions $\hat{\boldsymbol{\alpha}}$ to form the error sequence $\boldsymbol{\varepsilon}$. It is assumed that all decisions are correct, i.e. $\hat{\boldsymbol{\alpha}} = \boldsymbol{\alpha}$, where $\boldsymbol{\alpha}$ and $\hat{\boldsymbol{\alpha}}$ are the delayed versions of the input and quantized estimate, respectively:

$$\boldsymbol{\alpha}(D) = \boldsymbol{a}(D)\boldsymbol{\Delta}(D) \quad (41)$$
$$\hat{\boldsymbol{\alpha}}(D) = \hat{\boldsymbol{a}}(D)\boldsymbol{\Delta}(D). \quad (42)$$

According to Figure 10, the output of the delay matrix $\tilde{\boldsymbol{\alpha}}$ can be written as

$$\tilde{\boldsymbol{\alpha}}(D) = [\boldsymbol{a}(D)\boldsymbol{S}_x(D) + \boldsymbol{z}(D)]\,\boldsymbol{W}(D)\boldsymbol{\Delta}(D). \quad (43)$$

Since all decisions are assumed to be correct, the error signal after the delay matrix is given by

$$\boldsymbol{\varepsilon} = \tilde{\boldsymbol{\alpha}} - \boldsymbol{\alpha}. \quad (44)$$

This error signal serves as input to a prediction filter matrix $\boldsymbol{P}$ that tries to extrapolate the value of $\boldsymbol{\varepsilon}$ at the next time. The prediction

$$\tilde{\boldsymbol{\varepsilon}}(D) = \boldsymbol{\varepsilon}(D)\boldsymbol{P}(D) \quad (45)$$

is subtracted from the linear estimate $\tilde{\boldsymbol{\alpha}}$, which yields a better unquantized estimate

$$\bar{\boldsymbol{\alpha}} = \tilde{\boldsymbol{\alpha}} - \tilde{\boldsymbol{\varepsilon}}. \qquad (46)$$

The linear filter matrices $\boldsymbol{W}(D)$ and $\boldsymbol{P}(D)$ are chosen such that the mean-squared magnitude of the error

$$\boldsymbol{\epsilon} = \bar{\boldsymbol{\alpha}} - \boldsymbol{\alpha} \qquad (47)$$

is minimized. It can be shown, [10], that the optimum forward filter matrix is identical to that of the linear MMSE E/C, i.e.

$$\boldsymbol{W}(D) = \boldsymbol{L}(D) \qquad (48)$$

where $\boldsymbol{L}(D)$ is given by Equation (29). The predictor $\boldsymbol{P}(D)$ has to be a *purely causal* matrix filter [6], i.e. $\boldsymbol{P}(D) = \boldsymbol{P}[0] + \boldsymbol{P}[1]D^1 + \boldsymbol{P}[2]D^2 + \cdots$, and $\boldsymbol{P}[0]$ is restricted to be an upper triangular matrix with zeros along the diagonal. It is possible to calculate the infinite-length predictor in the D-domain using a computationally complex spectral factorization [10], [9]. Alternatively, the finite-length predictor may be determined [10]. This procedure requires the inversion of at least one matrix with the dimension $(NL_p - 1)$, where L_p is the length of the predictor.

Let us finally define the *error spectrum*

$$\boldsymbol{S}_\varepsilon(D) = E_M\left[\boldsymbol{\varepsilon}^H(D^{-*})\boldsymbol{\varepsilon}(D)\right]. \qquad (49)$$

Substituting Eqns. (41), (43), (44) into (49), considering (30), (37), (38) and using (29), the error spectrum can be expressed as

$$\boldsymbol{S}_\varepsilon(D) = \boldsymbol{\Lambda}(D) \qquad (50)$$

where $\boldsymbol{\Lambda}(D)$ is defined by

$$\boldsymbol{\Lambda}(D) = \boldsymbol{\Delta}^{-1}(D)\boldsymbol{L}(D)\boldsymbol{\Delta}(D). \qquad (51)$$

E. Parallel Structure (MNP-DFE)

A special case of the MNP-DDFE is obtained for $\boldsymbol{\Delta}(D) = \boldsymbol{I}_N$, i.e. taking out the delay elements after the forward filter matrix. This structure is called the multivariate noise-predictive decision-feedback equalizer (MNP-DFE) [9].

F. Successive Structure (MNE-DDFE)

The successive MNP-DDFE delays each sequence infinitely long with respect to the previous user's sequence. In practice, infinite delays are not necessary. It is sufficient to choose the delays large enough such that the interference from one user's signal into another can be almost completely estimated. However,

for analytical purposes, infinite delays are assumed in the following.

Consider a multiuser system with N users. The system model for an MNP-DDFE receiver is shown in Figure 10. The successive equalizer structure is now defined in the following way: Each sequence a_k $(k = 2, \ldots, N)$ is delayed infinitely with respect to the sequence a_{k-1} by the decision element D^{Δ_k}. In other words, before the decision on symbol $a_k[n_0]$ is made, the sequences $a_m[n]$ $(m = 1, \ldots, k - 1)$ are known for all values of $n \in (-\infty, \infty)$. Additionally, the previous symbols $a_k[n]$ of the current sequence are known for all $n \in (-\infty, n_0 - 1]$. This information might be used in the feedback filter.

Let us define the error signal after the forward filter matrix as

$$e_i = \tilde{a}_i - a_i, \quad i \in [1, N]. \qquad (52)$$

Additionally, we introduce the error vectors

$$\boldsymbol{e}_i = [e_1, e_2, \ldots, e_i] \qquad (53)$$
$$\boldsymbol{e} = \boldsymbol{e}_N. \qquad (54)$$

Considering Equations (40), (41) and (44), it can easily be seen that $\boldsymbol{\varepsilon}$ is a delayed version of $\boldsymbol{e}$:

$$\boldsymbol{\varepsilon}(D) = \boldsymbol{e}(D)\boldsymbol{\Delta}(D). \qquad (55)$$

Using Equation (50), the spectrum of $\boldsymbol{e}$ is given by

$$\boldsymbol{S}_e(D) = E_M\left[\boldsymbol{e}^H(D^{-*})\boldsymbol{e}(D)\right] = \boldsymbol{L}(D). \qquad (56)$$

The spectrum of the error vector $\boldsymbol{e}_i$ shall be denoted with

$$\boldsymbol{L}_i(D) = E_M\left[\boldsymbol{e}_i^H(D^{-*})\boldsymbol{e}_i(D)\right], \quad i \in [1, N]. \qquad (57)$$

Note that the submatrix $\boldsymbol{L}_i(D)$ is obtained by taking the first i rows and columns of $\boldsymbol{L}(D)$. Let us further define the inverse filter matrices

$$\boldsymbol{G}_i(D) = \boldsymbol{L}_i^{-1}(D), \quad i \in [1, N]. \qquad (58)$$

For $i = N$ we can write

$$\boldsymbol{L}(D) = \boldsymbol{L}_N(D) \qquad (59)$$
$$\boldsymbol{G}(D) = \boldsymbol{G}_N(D). \qquad (60)$$

According to the Definitions (57) and (53), $\boldsymbol{L}_i(D)$ can be partitioned for $i = 2, \ldots, N$ into

$$\boldsymbol{L}_i(D) = \begin{bmatrix} \boldsymbol{L}_{i-1}(D) & \boldsymbol{\lambda}_i^H(D) \\ \boldsymbol{\lambda}_i(D) & l_i(D) \end{bmatrix} \qquad (61)$$

where

$$\boldsymbol{\lambda}_i(D) = E_M\left[e_i^*(D^{-*})\boldsymbol{e}_{i-1}(D)\right] \qquad (62)$$
$$l_i(D) = E_M\left[e_i^*(D^{-*})e_i(D)\right] \qquad (63)$$

Furthermore, $\boldsymbol{G}_i(D)$ shall be partitioned into the following elements:

$$\boldsymbol{G}_i(D) = \begin{bmatrix} \boldsymbol{\Gamma}_i(D) & \boldsymbol{\gamma}_i^H(D) \\ \boldsymbol{\gamma}_i(D) & g_i(D) \end{bmatrix}. \qquad (64)$$

Instead of exploiting all possible information, the subsequently described method uses only the two-sided sequences

$$a_m[n], \quad m \in [1, k-1], \quad n \in (-\infty, \infty) \qquad (65)$$

while the symbols of the one-sided sequence $\{a_k[n]|n \in (-\infty, n_0 - 1]\}$ are discarded. The problem is therefore to estimate the error signal e_k in terms of the sequences e_m ($m \in [1, k-1]$). Since these sequences are two-sided, i.e. known for all values from $-\infty$ to ∞, the estimation problem can easily be solved in the D-domain. Especially, spectral factorization is not required.

A linear filter shall be used to determine the error estimate $\tilde{e}_k$. Let us assume that all previous decisions are correct. In this case, we know exactly the error sequences e_m ($m \in [1, k-1]$). These signals serve as inputs to the estimator. Using the error vector (53), the error estimate $\tilde{e}_k$ can be calculated in the D-domain with

$$\tilde{e}_k(D) = \boldsymbol{e}_{k-1}(D)\boldsymbol{p}_k^H(D^{-*}) \qquad (66)$$

where $\boldsymbol{p}_k^H(D^{-*})$ is the transfer vector function of the linear estimator. The estimation error is defined as difference between the real error e_k and the estimate $\tilde{e}_k$:

$$\epsilon_k = e_k - \tilde{e}_k. \qquad (67)$$

Our objective is to find the linear transformation $\boldsymbol{p}_k^H(D^{-*})$ which minimizes the expectation of the mean-squared error $|\epsilon_k[n]|^2$. The optimal estimator has to fulfill the orthogonality principle

$$E\left[\epsilon_k^*[n]\boldsymbol{e}_{k-1}[m]\right] = \boldsymbol{o}_{k-1}, \quad \forall n, m \in Z \qquad (68)$$

where $\boldsymbol{o}_v = [0, 0, \dots, 0]$ is the $1 \times v$ zero vector and Z denotes the set of integer numbers. Condition (68) can be formulated equivalently in the D-domain as

$$E_M\left[\epsilon_k^*(D^{-*})\boldsymbol{e}_{k-1}(D)\right] = \boldsymbol{o}_{k-1}. \qquad (69)$$

Substituting Eqns. (67), (66) into (69), solving for $\boldsymbol{p}_k$ and using the Definitions (57), (58), (61) yields

$$\boldsymbol{p}_k(D) = \boldsymbol{\lambda}_k(D)\boldsymbol{G}_{k-1}(D). \qquad (70)$$

The filter matrices $\boldsymbol{G}_k = \boldsymbol{L}_k^{-1}$ may be calculated recursively with [19, pp. 445–46]

$$\boldsymbol{G}_{k-1}(D) = \boldsymbol{\Gamma}_k(D) - \frac{1}{g_k}\boldsymbol{\gamma}_k^H(D)\boldsymbol{\gamma}_k(D) \qquad (71)$$

where $k = 2, \dots, N$. Therefore, the matrices $\boldsymbol{G}_k$ can be easily and efficiently computed by starting with $\boldsymbol{G}_N(D) = \boldsymbol{G}(D)$ and recursively solving Equation (71). The start matrix $\boldsymbol{G}(D) = \boldsymbol{L}^{-1}(D)$ can be obtained from Equation (29)

$$\boldsymbol{G}(D) = \boldsymbol{S}_x(D) + \boldsymbol{S}_a^{-1}(D). \qquad (72)$$

Note that there are no matrix inversions required during the calculation of the optimal feedback matrix filters.

Since the error estimate is estimated from the complete two-sided error sequences of previous users rather than predicted from temporally preceding symbols, the successive feedback structure described here will be called *multivariate noise-estimation delayed-decision-feedback equalizer* (MNE-DDFE). It has to be mentioned that if the structure shown in Figure 10 is used to realize the MNE-DDFE, appropriate delays will be necessary in front of the feedback filter matrix. The reason is that the input to the feedback estimator $\boldsymbol{p}_k$ has to be the error vector $\boldsymbol{e}_{k-1}$ or a delayed version of it.

Before an expression for the normalized MMSE (NMMSE) is derived, let us assume that the input signals a_i are mutually independent and that samples of the same sequence are uncorrelated with zero mean and variance $\mathcal{E}_a$, i.e. Equation (32) is fulfilled. Thus, the spectrum of the input signal reduces to $\boldsymbol{S}_a(D) = \mathcal{E}_a \boldsymbol{I}_N$. The NMMSE of the k-th user is defined by

$$\sigma_{\mathrm{mne},k} = 1/\mathcal{E}_a\, E\left[|\bar{a}_k[n] - a_k[n]|^2\right] \qquad (73)$$

which can easily be shown to be equal to the estimation error of the feedback filter matrix:

$$\sigma_{\mathrm{mne},k} = 1/\mathcal{E}_a\, E\left[|e_k[n] - \tilde{e}_k[n]|^2\right]$$
$$= 1/\mathcal{E}_a\, E\left[|\epsilon_k[n]|^2\right]. \qquad (74)$$

Let us define the spectrum of $\boldsymbol{\epsilon} = [\epsilon_1, \epsilon_2, \dots, \epsilon_N]$ as

$$\boldsymbol{S}_\epsilon(D) = E_M\left[\boldsymbol{\epsilon}^H(D^{-*})\boldsymbol{\epsilon}(D)\right]. \qquad (75)$$

The k-th diagonal element of $\boldsymbol{S}_\epsilon(D)$ is given by

$$S_{\epsilon,kk} = E_M\left[\epsilon_k^*(D^{-*})\epsilon_k(D)\right]. \qquad (76)$$

Expanding (76) using (67), (66), (57), (62), (63) and the fact that for the optimum MNE-DDFE relation (70) is fulfilled yields

$$S_{\epsilon,kk}(D) = L_{kk}(D) - \boldsymbol{\lambda}_k(D)\boldsymbol{G}_{k-1}(D)\boldsymbol{\lambda}_k^H(D^{-*}). \qquad (77)$$

The normalized MMSE of the k-th user is now obtained by evaluating $S_{\epsilon,kk}$ on the unit circle and integrating over the normalized frequency $\check{f} = fT_s$ from

0 to 1:

$$\sigma_{\text{mne},k} = \frac{1}{\mathcal{E}_a} \int_0^1 S_{\epsilon,kk}(e^{-j2\pi\check{f}})\, d\check{f}. \qquad (78)$$

Substituting (77) into (78) and considering the relation (35) we obtain

$$\sigma_{\text{mne},k} = \sigma_{\text{lin},k} - \frac{1}{\mathcal{E}_a} \int_0^1 \boldsymbol{\lambda}_k(D)\boldsymbol{G}_{k-1}(D)\boldsymbol{\lambda}_k^H(D^{-*})\, d\check{f} \qquad (79)$$

where $D = e^{-j2\pi\check{f}}$ and $\sigma_{\text{lin},k}$ is the NMMSE of user k for a linear MMSE equalizer/combiner.

IV. Numerical results

The numerical results have been obtained for the system shown in Figure 1 with the following parameters:

- Symbol period $T = 50$ ns,
- Number of receive antennas $A = 4$,
- Oversampling factor $K = 4$.

Therefore, the degree of diversity is equal to $AK = 16$. As long as no more than 16 users are present, the system is referred to as *well populated*. If the number of users exceeds the degree of diversity, we will call the system *overpopulated*. The number of system users N has been varied between 1 and 30. Identical fifth-order butterworth lowpass filters with cut-off frequency $f_c = K/(2T)$ have been chosen for the analog transmit and receive filters $p_C(t)$ and $b_C(t)$. The discrete-time transmit filters of all users have been set to $q_i[n] = \delta[n]$. In other words, the filters q_i have been omitted completely.

Measured channel impulse responses (CIR) have been used in the calculation of the numerical values. The CIR's have been measured in an indoor office environment at TR*Labs* [20]. The measurement system included four stationary transmit antennas and a mobile with four receive antennas. The distance between two adjacent receive antennas was one wavelength of the carrier frequency $f_{\text{car}} = 1.8$ GHz. The stationary antennas were placed in different corners of the office environment. Different impulse responses were obtained by changing the location of the mobile. Each measurement at a certain mobile location yielded four sets of four CIR's between the adjacent mobile antennas and one of the stationary antennas. The four CIR's belonging to one set had the same large scale propagation characteristics because the distances between a certain stationary antenna and each of the four mobile antennas were practically the same. The measurements resulted in a total of 2044 sets or 8176 CIR's. The bandwidth of the measured CIR's was approximately 120 MHz.

The reverse link of the system has been simulated by randomly selecting 30 out of 2044 CIR sets and assigning each to one of 30 users. The users have been divided into several groups of N portables for which the theoretical MMSE's (35) and (79) have been calculated. This procedure has been repeated 100 times for each value of N with different CIR sets.

The received SNR for an individual user shall here be defined as

$$\text{SNR}_i = \sum_{l=1}^{A} \frac{E_{i,l}}{N_0} \qquad (80)$$

where $E_{i,l}$ is the at base antenna l received average energy per symbol transmitted by user i, and N_0 is the two-sided power spectral density of the complex AWGN signals ν_{CGl}.

The linear MMSE E/C as well as the parallel (MNP-DFE) and successive (MNE-DDFE) decision-feedback equalizers are compared in Figures 11 and 12. These figures show the performance of the worst and the best of the 30 selected users, averaged over all 100 trials. The results are displayed in terms of the MMSE versus the number of simultaneously transmitting users. Figure 11 shows a situation where the average received signal-to-noise ratio (SNR) is 30 dB. The individual received SNR's are varying by up to ± 5 dB around the average SNR. The figure shows thus a situation of no or less stringent power control in which the individual received SNR's between the strongest and weakest user differ by 10 dB. The results show that both decision-feedback structures perform significantly better than the linear equalizer. The worst user MMSE of the successive DFE (MNE-DDFE) is lower than that of the parallel DFE (MNP-DFE) in the well populated region ($N \leq 16$). In contrast, the best system user performs better with an MNP-DFE receiver. This behavior is expected because the MNE-DDFE estimates the error of the weakest signal from all decisions of the other signals. In contrast, the MNP-DFE can only use decisions on temporally preceding symbols, but not following symbols since their decisions are made at a later time. Consequently, the feedback filter of the MNE-DDFE has more information (approximately twice as much) that can be used to estimate the error signal of the weakest user than the MNP-DFE. The noise estimate of the MNE-DDFE is therefore on average more accurate and leads to a better performance of the worst user. The situation is different for the strongest user. In this case, no decisions are available for the noise estimation of the MNE-DDFE. The MNP-DFE, however, is able to use the decisions of all temporally preceding symbols, as in the case of any other user.
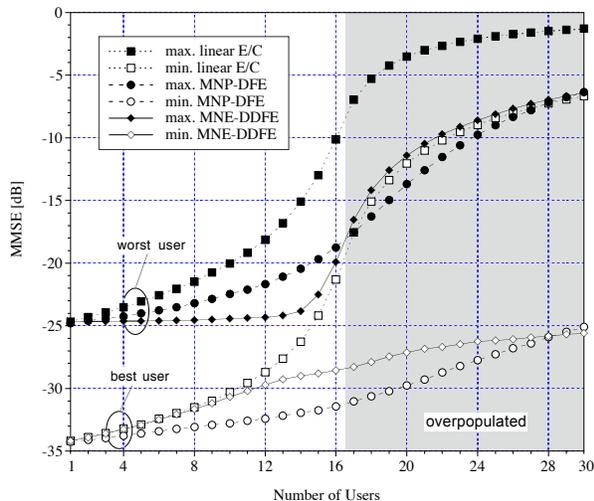
Fig. 11. MMSE for linear E/C, MNP-DFE and MNE-DDFE (received SNR's per user varying by up to 10 dB).
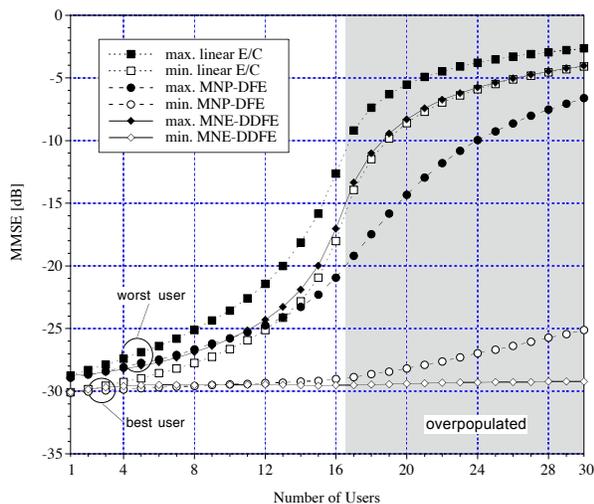
Fig. 12. MMSE for linear E/C, MNP-DFE and MNE-DDFE (received SNR's per user varying by up to 1 dB).

Therefore, a noise estimate is available and reduces the MMSE.

The results shown in Figure 12 have been obtained for a maximal ± 0.5 dB variation of the individual received SNR's around an average received SNR of 30 dB. Apart from that, exactly the same frequency responses have been used in the calculation of the MMSE as in the previous figure. The situation can be viewed as one of almost perfect power control. As before, both DFE receivers outperform the linear MMSE E/C. Let us concentrate on the worst user because this is the main performance limiting factor for the whole system. For a small number of users, the MMSE of both delayed and non-delayed DFE structures is almost identical. The worst user

MMSE of the MNE-DDFE is lower bounded by the best user MMSE of the linear equalizer. These two curves are very close for more than 12 users. Comparing all three receivers, the worst user MMSE of the MNP-DFE shows the best performance if we consider a larger population. The MMSE difference becomes significant in overpopulated systems where the worst user difference is as large as 5 dB. It has to be noted, however, that these results neglect the effects of wrong decisions on the results. In practice, error propagation may occur. To prevent a pathological scenario, the MSE at the output of the linear forward filter and at the output of the quantizers have to be monitored in order to detect error propagation. When error propagation occurs, the outputs of the linear forward filter, which is in fact a linear MMSE E/C, have to be fed directly into the quantizers without subtracting erroneous noise estimates from the feedback filters. This mode has to be continued until the memory of the feedback filters is filled completely with decisions of the linear estimate. After that, the feedback subtraction can be switched on again. However, this strategy can only be successful when the linear estimates are sufficiently reliable. Consequently, the DFE receivers rely on an acceptable performance of the linear MMSE E/C. If we consider -10 dB as minimum MSE requirement for the linear forward filter, overpopulated situations should be avoided. Thus, the advantage of the MNP-DFE over the MNE-DDFE in overpopulated systems may not be exploited in practice. In essence, both DFE receivers have for practical purposes almost the same worst user performance. This is also true if we consider the best users in the system.

The difference between the MNP-DDFE and MNE-DDFE is that the former uses finite delays while the latter delays one sequence infinitely with respect to another. The objective is now to compare the performance of an MNP-DDFE with relatively long individual delays and an MNE-DDFE. The individual delays of the MNP-DDFE have been chosen to $\Delta_1 = 0$ and $\Delta_k = \Delta_{k-1} + 3$ for $k = 2, 3, \ldots, N$, i.e. the signal of user k is delayed by 3 symbols relative to the signal of user $k - 1$. The length of the feedback filters has been set to $L_p = 7$. In order to reduce the dimension of the matrices to be inverted, a reduced complexity version of the MNP-DDFE is used [10]. One simplification is achieved by feeding into the predictor only the error signals from users with a better performance after the linear forward filter, i.e. for user k only the signals $\hat{a}_i$ for $i = 1, 2, \ldots, k$ are fed back while decisions of the signals $\hat{a}_j$ $(j = k + 1, \ldots, N)$ are discarded.

This should reduce the performance only slightly because the worse sequences are delayed by at least 3 symbols and have a negligible influence on the estimated noise value. The second complexity reduction is achieved by inserting for every user a different delay matrix $\mathbf{\Delta}_{P,k} = \mathbf{D}\mathrm{iag}\langle D^{\max\{3(k-i-1);0\}}\rangle$ $(i = 1, \ldots , k)$ in front of the predictor. This guarantees that the quantized sequences of all better users are delayed by exactly 3 symbols and reduces the matrix dimensions significantly [10]. It was observed that this resulted in a negligible performance degradation. The difference between the MNE-DDFE and the reduced-complexity MNP-DDFE used in our investigation can be summarized as follows:

• The MNE-DDFE delays the sequence of one user infinitely with respect to the next user. The MNP-DDFE introduces relative delays of 3 symbols.
• Past decisions of the same sequence are used in the feedback loop of the MNP-DDFE. However, the MNE-DDFE does not use available decisions of the same sequence.
• The feedback part of the MNE-DDFE uses infinite-length filters, while the feedback filters of the MNP-DDFE are restricted to a finite length (in this case $L_p = 7$).

The relative delay of 3 symbols between two consecutive sequences enables the MNP-DDFE to use almost all CCI causing symbols of the better signals in the noise estimation process. The characteristic of the channel is such that symbols sent more than 3 symbol periods before or after the current ones cause only negligible ISI or CCI in the current symbols. The MNP-DDFE behaves therefore in this case almost like an ideal successive equalizer. It is thus expected that the described MNP-DDFE and the MNE-DDFE show a very similar performance. The obtained results confirm this. Figure 13 shows the ratio of the MMSE for the MNE-DDFE to the MMSE of the MNP-DDFE in dB for different numbers of users in the system. The MMSE values of the MNP-DDFE have been obtained with the method and expression described in Reference [10]. The average received SNR of all users was chosen as before to 30 dB and the individual received SNR's vary by up to 10 dB between the best and worst users. One curve shows the ratio for the worst user, another curve is the MMSE ratio of the best user and the crosses represent the average ratio over all system users. A positive value indicates that the MMSE of the MNP-DDFE is smaller while negative values mean that the MNE-DDFE performs better. As expected, both equalizer types perform almost identical in the well populated region. For 16 users, the MNP-DDFE has a better worst user performance
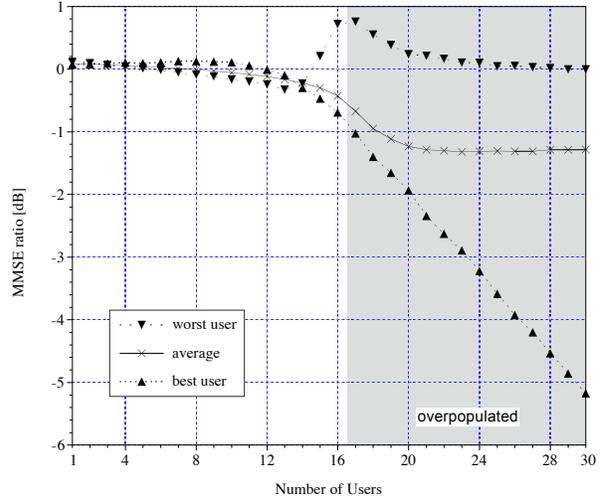
Fig. 13. Ratio of the MMSE between MNE-DDFE and MNP-DDFE over the number of system users.

of roughly 0.8 dB. This may be contributed to the fact that the MNP-DDFE uses past decisions of the same sequence in the estimation process while the MNE-DDFE does not. This additional information becomes more important when all degrees of freedom are used for interference suppression and there is no diversity left. For more than 16 users, the better worst user performance of the MNP-DDFE decreases and vanishes eventually. On the other hand, the average and best user MMSE of the MNE-DDFE is smaller. The ratio is larger in the overpopulated region. This may be contributed to the fact that the feedback filters of the MNE-DDFE are of infinite length while the MNP-DDFE is restricted to $L_p = 7$ taps. The larger MMSE difference for a higher number of transmitting system users might not be important under practical considerations. It has to be mentioned again in this context that both DFE structures may not perform good enough in overpopulated systems because of potential problems due to error propagation.

V. CONCLUSIONS

In this work, the topic of multiuser equalization has been treated in a general form. The focus has been on delayed-decision-feedback equalizers. We started out with the description of several equivalent structures of the linear MMSE equalizer/combiner (E/C). One of these structures led to the derivation of an equivalent discrete-time system model. The order in which the decisions are made becomes important when detectors are considered that feed these decisions back into the receiver. One way to describe the decision order is by means of the deci-

sion path. With this concept, the delayed-decision-feedback equalizer may be viewed as a detector that enables a more flexible order in which the symbols of different sequences are quantized. It has been shown that the decision order determines the properties of the delayed DFE and changes the performance of the detected signals transmitted from different users. It is possible to trade-off a better performance of one user with a worse performance of another. This might improve the overall system performance especially when the error rate of different signals differs considerably. We have described two different implementations of the delayed DFE, namely the M-DDFE and the MNP-DDFE. The MNP-DDFE has been analyzed in greater detail. The parallel and successive versions of the MNP-DDFE are special cases in which the delay parameters are chosen to be zero and infinite, respectively. The successive structure, denoted MNE-DDFE, leads to a simple estimation problem that has been solved in the D-domain. The feedforward part of the MNE-DDFE (and MNP-DDFE) is equal to the linear MMSE E/C. It has been shown that the feedback filter matrix of the successive equalizer can be easily determined without computationally involving methods like spectral factorization or matrix inversion. The numerical results showed evidence for a superior performance of the successive DFE in situations when the received signal powers of different users vary by up to 10 dB. If the signals are received with almost equal power, both the successive and parallel structures show a comparable performance as long as the number of users does not exceed the practical limit.

References

[1] Sergio Verdú, "Minimum probability of error for asynchronous Gaussian multiple-access channels," *IEEE Trans. Inform. Theory*, vol. IT-32, no. 1, pp. 85–96, Jan. 1986.

[2] Sergio Verdú, "Optimum multiuser asymptotic efficiency," *IEEE Trans. Commun.*, vol. COM-34, no. 9, pp. 890–897, Sept. 1986.

[3] Ruxandra Lupas and Sergio Verdú, "Linear multiuser detectors for synchronous code-division multiple-access channels," *IEEE Trans. Inform. Theory*, vol. 35, no. 1, pp. 123–136, Jan. 1989.

[4] Zhenhua Xie, Robert T. Short, and Craig K. Rushforth, "A family of suboptimum detectors for coherent multiuser communications," *IEEE J. Select. Areas Commun.*, vol. 8, no. 4, pp. 683–690, May 1990.

[5] M. L. Honig, P. Crespo, and K. Steiglitz, "Suppression of near- and far-end crosstalk by linear pre- and post-filtering," *IEEE J. Select. Areas Commun.*, vol. 10, no. 3, pp. 614–629, Apr. 1992.

[6] Alexandra Duel-Hallen, "Equalizers for multiple input/multiple output channels and PAM systems with cyclostationary input sequences," *IEEE J. Select. Areas Commun.*, vol. 10, no. 3, pp. 630–639, Apr. 1992.

[7] Brent R. Petersen and David D. Falconer, "Minimum mean-square equalization in cyclostationary and stationary interference – analysis and subscriber-line calculations," *IEEE J. Select. Areas Commun.*, vol. 9, no. 6, pp. 931–940, Aug. 1991.

[8] Alexandra Duel-Hallen, "Decorrelating decision-feedback multiuser detector for synchronous code-division multiple-access channel," *IEEE Trans. Commun.*, vol. 41, no. 2, pp. 285–290, Feb. 1993.

[9] Evangelos Eleftheriou and Brent R. Petersen, "Method and apparatus for multiuser-interference reduction," World Intellectual Property Organization, Aug. 1995, International Patent No. WO 95/22209.

[10] Ramon Schlagenhaufer, Brent R. Petersen, and Abu B. Sesay, "The multivariate noise-predictive delayed-decision-feedback equalizer/combiner for multiuser systems with diversity," in *Conf. Rec. IEEE CCECE 99*, Edmonton, AB, Canada, May 1999, pp. 39–44.

[11] M. K. Varanasi and B. Aazhang, "Multistage detection in asynchronous code division multiple-access communications," *IEEE Trans. Commun.*, vol. COM-38, no. 4, pp. 509–519, Apr. 1990.

[12] A. J. Viterbi, "Very low rate convolutional codes for maximum theoretical performance of spread spectrum multiple access channels," *IEEE J. Select. Areas Commun.*, vol. 8, no. 4, pp. 641–649, May 1990.

[13] Jack Holtzman, "DS/CDMA successive interference cancellation," in *Proc. of ISSSTA'94*, Oulu, Finland, July 1994, pp. 69–78.

[14] Glenn D. Golden, "Cancellation of synchronous cyclostationary interference (SCI) using fractionally spaced equalizers," invited Seminar, Dept. of Systems and Computer Engineering, Carleton University, Ottawa, Ont., K1S 5B6, Mar. 1990.

[15] William A. Gardner, "Cyclic Wiener filtering: Theory and method," *IEEE Trans. Commun.*, vol. 41, no. 1, pp. 151–163, Jan. 1993.

[16] Brent R. Petersen and David D. Falconer, "Suppression of adjacent-channel, cochannel and intersymbol interference by equalizers and linear combiners," *IEEE Trans. Commun.*, vol. 42, no. 12, pp. 3109–3118, Dec. 1994.

[17] Ramon Schlagenhaufer, Abu B. Sesay, and Brent R. Petersen, "A wireless multiuser system using diversity," in *Conf. Rec. IEEE VTC 99*, Houston, Texas, May 1999, pp. 2024–2028.

[18] Mohsen Kavehrad and Jack Salz, "Cross-polarization cancellation and equalization in digital transmission over dually polarized multipath fading channels," *AT&T Techn. J.*, vol. 64, no. 10, pp. 2211–2245, Dec. 1985.

[19] Rudolf Zurmühl and Sigurd Falk, *Matrizen und ihre Anwendungen 1*, vol. 1, Springer, Berlin Heidelberg New York, seventh edition, 1997, in German.

[20] Rayhan Behin, "Multi-antenna indoor radio channel measurement and analysis," Technical report, TR*Labs*, Calgary, AB, Canada, May 1998.